doi:10.1093/brain/awt271 Brain 2013: 136; 3659–3670 | 3659

BRAIN
A JOURNAL OF NEUROLOGY

A direct relationship between oscillatory subthalamic nucleus–cortex coupling and rest tremor in Parkinson's disease

Jan Hirschmann,[1,2] Christian J. Hartmann,[1,2] Markus Butz,[1,3] Nienke Hoogenboom,[1,2] Tolga E. Özkurt,[4] Saskia Elben,[1,2] Jan Vesper,[5] Lars Wojtecki[1,2] and Alfons Schnitzler[1,2]

1 Institute of Clinical Neuroscience and Medical Psychology, Medical Faculty, Heinrich-Heine-University Düsseldorf, Düsseldorf, Germany
2 Department of Neurology, University Hospital Düsseldorf, Düsseldorf, Germany
3 Sobell Department of Motor Neuroscience and Movement Disorders, Institute of Neurology, University College London, London, UK
4 Department of Health Informatics, Informatics Institute, Middle East Technical University, Ankara, Turkey
5 Department of Functional Neurosurgery and Stereotaxy, University Hospital Düsseldorf, Düsseldorf, Germany

Correspondence to: Alfons Schnitzler
Institute of Clinical Neuroscience and Medical Psychology
Heinrich-Heine-University Düsseldorf
Universitätsstr. 1
D-40225 Düsseldorf
Germany
E-mail: SchnitzA@med.uni-duesseldorf.de

Electrophysiological studies suggest that rest tremor in Parkinson's disease is associated with an alteration of oscillatory activity. Although it is well known that tremor depends on cortico-muscular coupling, it is unclear whether synchronization within and between brain areas is specifically related to the presence and severity of tremor. To tackle this longstanding issue, we took advantage of naturally occurring spontaneous tremor fluctuations and investigated cerebral synchronization in the presence and absence of rest tremor. We simultaneously recorded local field potentials from the subthalamic nucleus, the magnetoencephalogram and the electromyogram of forearm muscles in 11 patients with Parkinson's disease (all male, age: 52–74 years). Recordings took place the day after surgery for deep brain stimulation, after withdrawal of anti-parkinsonian medication. We selected epochs containing spontaneous rest tremor and tremor-free epochs, respectively, and compared power and coherence between subthalamic nucleus, cortex and muscle across conditions. Tremor-associated changes in cerebro-muscular coherence were localized by Dynamic Imaging of Coherent Sources. Subsequently, cortico-cortical coupling was analysed by computation of the imaginary part of coherency, a coupling measure insensitive to volume conduction. After tremor onset, local field potential power increased at individual tremor frequency and cortical power decreased in the beta band (13–30 Hz). Sensor level subthalamic nucleus-cortex, cortico-muscular and subthalamic nucleus-muscle coherence increased during tremor specifically at tremor frequency. The increase in subthalamic nucleus-cortex coherence correlated with the increase in electromyogram power. On the source level, we observed tremor-associated increases in cortico-muscular coherence in primary motor cortex, premotor cortex and posterior parietal cortex contralateral to the tremulous limb. Analysis of the imaginary part of coherency revealed tremor-dependent coupling between these cortical areas at tremor frequency and double tremor frequency. Our findings demonstrate a direct relationship between the synchronization of cerebral oscillations and tremor manifestation. Furthermore, they suggest the feasibility of tremor detection based on local field potentials and might thus become relevant for the design of closed-loop stimulation systems.

Received May 2, 2013. Revised July 4, 2013. Accepted August 2, 2013. Advance Access publication October 22, 2013

Keywords: Parkinson's disease; tremor; magnetoencephalography; coherence; deep brain stimulation

Abbreviations: DBS = deep brain stimulation; ImCoh = imaginary part of coherency; LFP = local field potential; MEG = magnetoencephalography

Introduction

Parkinson's disease is a debilitating neurological disorder resulting from progressive cell death of dopaminergic neurons in the midbrain (Lang and Lozano, 1998). Recent research revealed abnormally strong synchronization of rhythmic neuronal activity both in animal models of Parkinson's disease and patients, suggesting that Parkinson's disease is associated with pathologically altered neuronal oscillations (Schnitzler and Gross, 2005; Hammond *et al*., 2007). Enhanced synchronization was shown to play a role in akinesia and rigidity (Kühn *et al*., 2006) and was suggested to be involved in parkinsonian tremor.

Tremor occurs in ~75% of patients and may range from mild to severe manifestations (Hoehn and Yahr, 1967; Hughes *et al*., 1993). Classical parkinsonian tremor occurs at rest, and is attenuated at movement onset (Deuschl *et al*., 2000). Therefore, it is referred to as rest tremor. The frequency of parkinsonian rest tremor ranges between 3 and 7 Hz.

It is generally agreed that central rather than peripheral mechanisms underlie parkinsonian tremor (Elble, 1996; McAuley and Marsden, 2000; Schnitzler *et al*., 2006). Currently, two overlapping central networks are considered candidate generators: the cerebello-thalamo-cortical circuit and the basal ganglia-cortical motor loop (Helmich *et al*., 2012). Tremor-related neural activity occurs in both networks, and lesions and deep brain stimulation (DBS) of structures in either network lead to tremor suppression (Bergman *et al*., 1990; Benabid *et al*., 1991; Krack *et al*., 1997).

Patient recordings from the ventrolateral thalamus revealed coherence between single unit and muscle activity at tremor frequency, suggesting that the thalamus is involved in tremor generation (Lenz *et al*., 1988; Zirh *et al*., 1998). Moreover, the ventral intermediate nucleus of the thalamus is considered the most effective DBS target for tremor suppression (Deuschl *et al*., 2000). As this nucleus receives mainly cerebellar afferents, it was proposed that cerebellar activity also contributes to tremor expression (Stein and Aziz, 1999). In fact, imaging studies demonstrated that DBS of the ventral intermediate nucleus affects cerebellar blood flow and revealed that cerebellar blood oxygenation and metabolic activity are positively correlated with tremor amplitude (Deiber *et al*., 1993; Helmich *et al*., 2011; Mure *et al*., 2011).

Besides the cerebello-thalamic circuit, tremor research has focused on the basal ganglia. Microelectrode recordings in non-human primates (Raz *et al*., 2000; Heimer *et al*., 2006) and patients undergoing surgery (Hutchison *et al*., 1997) revealed so-called tremor cells in the internal globus pallidus. These cells fire bursts at tremor frequency and bursting is, at least transiently, coherent with tremor recordings from the muscle (Hurtado *et al*., 2005).

Similar observations were made in the subthalamic nucleus. In vervet monkeys, oscillations at tremor frequency and double tremor frequency emerged when the animals began to develop tremor due to 1-methyl-4-phenyl-1,2,3,6-tetrahydropyridine (MPTP) injection (Bergman *et al*., 1994). Furthermore, power spectra of subthalamic nucleus local field potentials (LFPs) show peaks at tremor frequency and subthalamic nucleus LFPs are coherent with the EMG at tremor frequency (Levy *et al*., 2002; Liu *et al*., 2002; Wang *et al*., 2005; Reck *et al*., 2009).

Notably, tremor-related oscillatory activity is not only found in subcortical nuclei and the cerebellum, but also in the cortex. Timmermann *et al*. (2003) studied cerebro-muscular coherence using magnetoencephalography (MEG) and observed significant coupling at tremor frequency and double the tremor frequency in a network including primary motor cortex, premotor cortex, posterior parietal cortex, cerebellum and a diencephalic source that was assumed to be the thalamus. The same network was later shown to underlie voluntary tremor in healthy controls (Pollok *et al*., 2004), and a similar network was found to be involved in essential tremor (Schnitzler *et al*., 2009).

In summary, several lines of evidence suggest that tremor manifestation is associated with cerebral oscillations at tremor frequency, indicating that they could serve as a trigger signal in closed-loop DBS (Rosin *et al*., 2011). The nature of this association, however, remains elusive. Patient studies on subthalamic nucleus single unit activity reported that rhythmic spiking around 5 Hz can be observed in the absence of tremor (Magariños-Ascone *et al*., 2000; Moran *et al*., 2008; Shimamoto *et al*. 2013). These results demonstrate that the presence of spectral peaks at tremor frequency is not sufficient to make inferences on the tremor state. Furthermore, they show that oscillations on the single cell level are not sufficient to elicit tremor, suggesting that tremor manifestation might require coordinated network activity.

In this study, we hypothesized that tremor depends on synchronization within the motor system. Specifically, we aimed at demonstrating that tremor is associated with modulations of subthalamic nucleus power, cortical power, subthalamic nucleus-cortex and cortico-cortical coupling. To this end, we simultaneously recorded subthalamic nucleus LFPs, MEG and the EMG of forearm muscles in tremor-dominant patients with Parkinson's disease. As demonstrated by several recent studies (Hirschmann *et al*., 2011, 2013; Litvak *et al*., 2011, 2012; Oswal *et al*., 2013), this combination of recording techniques is a powerful tool for studying connectivity between subthalamic nucleus, cortex and muscle. We identified epochs of spontaneous rest tremor as well as tremor-free epochs using the EMG recordings and compared oscillatory activity across conditions. The study critically extends our current knowledge about parkinsonian rest tremor by demonstrating the pivotal role of synchronous oscillations in subthalamic nucleus and cortex.

Materials and methods

Patients

Eleven patients with Parkinson's disease who were clinically selected for DBS because of levodopa-induced fluctuations and dyskinesias

Table 1 Clinical details of patients

Subject	Gender	Age (years)	Disease duration (years)	UPDRSIII recording day	Individual tremor frequency (hz)	Side	OFF/OFF upper limb rest tremor subscore	OFF/ON upper limb rest tremor subscore
1	M	65	8	40	4.0	Right	1	0
						Left	3	2
2	M	69	6	51	3.5	Right	3	3
						Left	3	2
3	M	68	11	36	3.0	Left	1	0
4	M	59	6	39	4.5	Right	3	1
						Left	3	0
5	M	68	2	39	4.0	Right	1	0
						Left	2	1
6	M	52	11	31	6.0	Right	2	0
						Left	0	0
7	M	67	6	34	6.5	Right	m.d.	m.d.
						Left	m.d.	m.d.
8	M	53	12	26	5.0	Left	2	2
9	M	65	4	43	4.5	Right	4	0
						Left	4	0
10	M	74	7	60	5.0	Right	4	0
11	M	69	12	30	7.0	Right	3	0
Mean		**64.45**	**7.73**	**39.00**	**4.82**		**2.40**	**0.60**
Standard deviation		**6.93**	**3.38**	**9.75**	**1.25**		**1.17**	**1.07**

The column labelled side indicates which body sides were analysed. The last two columns show the effect of deep brain stimulation on upper limb rest tremor as documented in the control assessment of motor symptoms ~3 months after implantation of the stimulation device. OFF/ON signifies that medication was off and stimulation was on (m.d. = missing data). M = male; UPDRS = Unified Parkinson's Disease Rating Scale.

participated in this study with written informed consent. All subjects suffered from moderate to severe rest tremor that was alleviated by DBS (Table 1). Seven subjects showed bilateral tremor during the recordings so that it was possible to include both hemispheres in the analysis. Four subjects showed unilateral tremor so that we were restricted to one hemisphere. Thus, 18 subthalamic nuclei were analysed in total. Subject 6 had been included in an earlier study on akinesia (Hirschmann *et al*., 2013). He showed transiently emerging tremor in addition to severe akinesia and rigidity. The study was approved by the local ethics committee (Study no. 3209) and is in accordance with the Declaration of Helsinki.

Surgery

Implantation of electrodes was carried out at the Department of Functional Neurosurgery and Stereotaxy of the University Hospital Düsseldorf. The surgical procedures are described elsewhere (Özkurt *et al*., 2011). Oral anti-parkinsonian medication was withdrawn the evening before surgery and substituted by subcutaneous apomorphine medication. Eight of 11 subjects were implanted with electrode model 3389 (Medtronic Inc.). Subjects 6, 8 and 9 were implanted with a DBS system by St. Jude Medical Inc. Electrode placement was guided by intraoperative microelectrode recordings, intraoperative stimulation and clinical testing of DBS efficacy.

Electrode contact localization

To reconstruct the final electrode placement, preoperative MRIs and postoperative CT scans were aligned using rigid transformation as provided by the functional magnetic resonance imaging of the Brain Linear Image Registration Tool (Jenkinson *et al*., 2012). Subsequently, the electrode position was derived from its characteristic artefacts in CT scans (Hemm *et al*., 2009). Contacts were labelled in a $0.5 \times 0.5 \times 0.5$ mm mask image in individual MRI space. For group comparison, individual MRI scans were transformed to Montreal Neurological Institute (MNI) space using the symmetric normalization strategy implemented in Advanced Normalisation Tools (Avants *et al*., 2008). The same transformation was applied to the mask images to obtain contact positions in MNI space.

Recordings

We simultaneously recorded LFPs from the subthalamic nucleus, MEG and the EMG of the extensor digitorum communis and flexor digitorum superficialis muscles of both upper limbs. All recordings were performed using a 306 channel, whole-head MEG system (Elekta Oy). The sampling rate was 2000 Hz. DBS electrodes were connected to the amplifier integrated into the MEG system by non-magnetic extension leads. Online filters were applied to create a passband of 0.03–660 Hz for MEG signals, and a passband of 0.1–660 Hz for LFP and EMG signals. EMG electrodes were referenced to surface electrodes at the muscle tendons. DBS electrodes were referenced to a surface electrode at the left mastoid and rearranged to a bipolar montage offline. Re-referencing was performed by signal subtraction and yielded three bipolar LFP channels per electrode: 0–1 (ventral), 1–2 and 2–3 (dorsal).

Clinical ratings and paradigm

Recordings took place the day after surgery. Two hours before recording apomorphine administration was stopped. The clinical OFF state was quantified by means of the motor score of the Movement Disorder Society Unified Parkinson's Disease Rating Scale immediately before the recording started (Goetz *et al*., 2008). The rating was performed by an experienced movement disorders specialist. Inside the

shielded room, subjects were instructed to sit as still as possible with eyes open. In the period analysed in this study, there was neither a task nor any kind of stimulus presentation. The duration of the rest recording varied according to the subsequent paradigm. Paradigm 1 (Subjects 1–8) included 10 min of rest in total and is described in detail in Hirschmann *et al*. (2013). Paradigm 2 (Subjects 9–11) included 3 min of rest.

Epoch selection

Raw data were inspected by eye. Epochs were labelled as tremor epochs if continuous 3–7 Hz periodic activity was clearly apparent in the EMG time series of both the upper limb extensor and flexor. Simultaneous tremor on the contralateral body side was not accounted for when determining tremor epochs, i.e. we did not differentiate between bilateral and unilateral tremor. Epochs were labelled as tremor-free only if neither forearm showed any periodic activity. Epochs containing artefacts such as contraction of jaw muscles or coughing were discarded. Data selection yielded 82 s of tremor-free data (range: 17–235 s) and 63 s of tremor data (range: 14–201 s) on average.

Preprocessing

Temporal Signal Space Separation (Taulu and Simola, 2006) was applied using MaxFilter (Elekta Oy) as a means to shield the MEG signal from tremor-related muscle activity. A discrete Fourier transform filter was applied to remove any remaining power line noise (50 Hz) and its first two harmonics (100 and 150 Hz). This processing step and all of the following were performed using Matlab R2012a (The Mathworks) and the FieldTrip toolbox (Oostenveld *et al*., 2011). EMGs were high-pass filtered at 10 Hz and full-wave rectified. Data were down-sampled to 256 Hz.

Channel selection

A set of 24 gradiometers contralateral to the tremulous limb was selected *a priori* as MEG sensors of interest. The sensors were chosen such that they covered sensorimotor and premotor motor cortex (Fig. 1A). The selection was adapted for each body side individually: in the sensors of interest, power was averaged over the individual tremor frequency band (tremor frequency ± 0.5 Hz) and the first harmonic band (double tremor frequency ± 0.5 Hz) and summed over conditions (tremor and tremor-free episodes). Subsequently, the sensor with maximum power and its six nearest neighbours were selected.

Furthermore, one LFP and one EMG channel were selected for each body side. For each of the three LFP channels contralateral to the tremulous limb, we computed LFP-MEG coherence and averaged across MEG channels of interest, resulting in one spectrum per LFP channel and condition. Coherence spectra from both conditions were summed, and we selected the LFP channel with highest coherence at individual tremor frequency for further analysis. Selection of the EMG channel of interest was performed analogously (either the forearm extensor or the forearm flexor of the tremulous limb was chosen). Fig. 1B shows the positions of selected LFP channels in MNI space together with a probability map of the subthalamic nucleus (Forstmann *et al*., 2012).

Sensor level analysis

Time-frequency representations

To investigate the dynamics of tremor-related LFP and MEG power at tremor onset, we selected all available tremor epochs with a discernible tremor onset that lasted $\geqslant 10$ s and were separated from the previous tremor epoch of the same limb by $\geqslant 10$ s. Time-frequency representations were produced by Fourier transformation of Hanning-tapered data in a sliding window that was moved in steps of 50 ms. Window length was set to 2 s for 1–4.5 Hz and to seven cycles for 5–30 Hz to obtain a better time resolution.

For statistical analysis, time-frequency representations were aligned to individual tremor frequency and compared to baseline (-9 to 0 s relative to tremor onset) using a non-parametric, cluster-based randomization approach (Maris and Oostenveld, 2007). In case multiple epochs were available for a single subthalamic nucleus, the corresponding time-frequency representations were averaged prior to statistical analysis. In short, a group statistical image was computed and two thresholds were applied. In this case, the thresholds were chosen to be the 0.05 and 0.95 percentiles of the distribution of the 'activation versus baseline *t*-value'. Following threshold application, values of neighbouring supra-threshold voxels were summed and the cluster sums were stored. Then, subject-specific images were randomly shuffled across conditions, an alternative statistical image was computed and cluster sums were computed as before. By repeating this step 1000 times, an empirical, non-parametric null distribution was constructed to which the original cluster sums were compared. Importantly, this approach effectively controls for multiple comparisons. Please note, however, that it does not account for possible statistical dependencies between hemispheres.

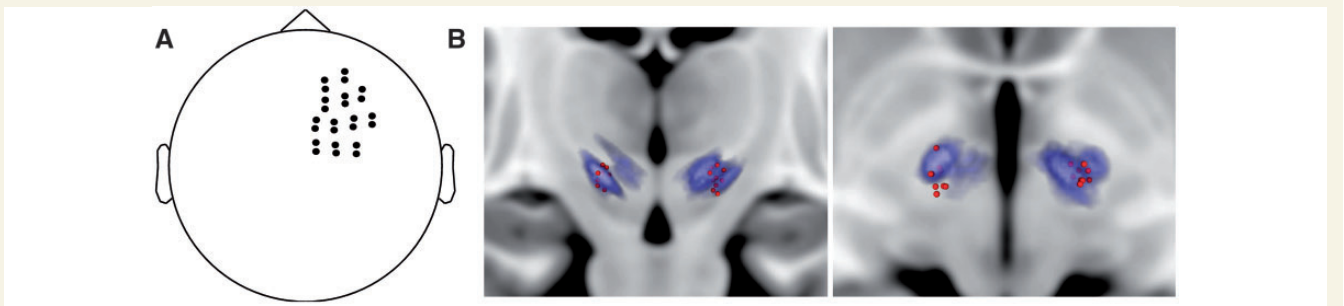

Figure 1 Location of selected channels. (**A**) *A priori* MEG sensor selection for subjects with left upper limb tremor. (**B**) Location of the selected LFP channels (red dots) in MNI space. The blue cloud represents a subthalamic nucleus probability map (Forstmann *et al*., 2012). Blue voxels belong to the subthalamic nucleus with a probability of $>4\%$. to belong to the subthalamic nucleus. *Left*: Coronal slice at $y = -17.5$ mm seen from anterior. *Right*: Axial slice at $z = -5.5$ mm seen from inferior.

Coherence spectra

For coherence analysis, data were divided into half-overlapping segments of 2-s length. Subsequently, data segments were arranged into two separate sets containing tremor and tremor-free episodes, respectively. Segments were convolved with a Hanning taper and coherence was calculated for both conditions. As in the analysis of power, coherence spectra were aligned to individual tremor frequency and compared across conditions using a non-parametric, cluster-based randomization approach. The dependent samples *t*-value served to define the cluster thresholds.

Correlation between EMG power and LFP-MEG coherence was quantified by Pearson's linear correlation coefficient. Power was considered in logarithmic units and coherence was Fisher *z*-transformed. In order to account for peaks at tremor frequency and at its first harmonic, we averaged coherence over the tremor frequency band and the first harmonic band prior to computing correlation.

Source analysis

Source analysis was performed using beamforming, a spatial filtering approach. Importantly, tremor and tremor-free epochs were both projected through a common, real-valued spatial filter that was derived from the joint data from both conditions. This step excludes the possibility that statistical differences between conditions occur due to differences in spatial filters.

Subthalamic nucleus-cortex and cortico-muscular coherence

Estimation of subthalamic nucleus-cortex and cortico-muscular coherence on the source level was realized by Dynamic Imaging of Coherent Sources (Gross *et al*., 2001). Regularization was set to 5% of the mean of the trace of the channel cross-spectral density matrix. Source orientation was defined as the orientation that maximized power. The forward model was based on a realistic, single shell head model derived from individual T_1-weighted structural MRIs (Nolte, 2003). The latter were obtained prior to surgery using a Magnetom Trio MRI scanner (Siemens). We made use of regular beamformer grids with 5 mm spacing that were aligned to MNI space (Mattout *et al*., 2007). All analysed beamformer grid points lay within 1.5 cm from the cortical surface, i.e. we did not consider subcortical structures. Limiting the analysis to cortical areas served to increase statistical power.

Statistical analysis of source level coherence was performed in the same way as for sensor level coherence. The non-parametric randomization approach is suited to analyse one-dimensional input, such as coherence spectra, as well as multi-dimensional input such as volumetric images (Maris and Oostenveld, 2007). A one-sided test was used as we explicitly sought to localize the coherence increases observed in the previous sensor level analysis.

Cortico-cortical coupling

For investigation of cortico-cortical coupling, the time domain activity of selected sources was reconstructed using a Linear Constraint Minimum Variance beamformer (Van Veen and Buckley, 1988). Regularization was set to 20%. To improve the signal-to-noise ratio, we made use of the FieldTrip implementation of the eigenspace beamformer approach (Sekihara *et al*., 2002). In this approach, a projection onto a subspace of the data covariance matrix is applied to remove noise components. We chose the subspace spanned by the first N singular vectors of the sensor covariance matrix with corresponding singular values σ_1 to σ_N, such that $\sigma_i / \sigma_1 > 0.2$ for all $i \in [1, 2, \ldots, N]$.

Following reconstruction of source time courses, we calculated coherence and the imaginary part of coherency (ImCoh) for all source pairs. ImCoh is a coupling measure related to coherence. Unlike coherence, it is unaffected by volume conduction and therefore better suited to investigate cortico-cortical coupling (Nolte *et al*., 2004). To improve the signal-to-noise ratio, the data were convolved with three Slepian tapers before analysing cortico-cortical coupling (Thomson, 1982).

Cortico-cortical coupling was statistically analysed using a repeated-measures ANOVA. The non-parametric randomization approach was not applied in this case since there is no established procedure to assess the influence of multiple factors. As in correlation analysis, coherence and ImCoh were averaged over the tremor frequency band and the first harmonic band. Coherence was Fisher *z*-transformed and ImCoh was rectified. The latter step ensured that subject-specific ImCoh values did not cancel in the group average. ANOVAs included the factors 'tremor' (no tremor, tremor), 'pair' (source X – source Y, source X – source Z, . . .) and 'shuffling' (original, shuffled). In the shuffled condition, one signal in each pair was shifted forward in time by k segments (circular shift). k was a random integer between 2 and $M - 1$, M being the total number of segments. We applied Greenhouse-Geisser correction for non-sphericity where appropriate.

Results

For each subject, we determined the individual tremor frequency. The latter was defined as the frequency of the first clear peak in the EMG power spectrum during tremor. Additional peaks at tremor frequency harmonics were observed in 15 cases. Individual tremor frequencies ranged between 3 and 7 Hz (Table 1). In every subject, individual tremor frequency was consistent across EMGs from different muscles and limbs.

Sensor level power

We investigated changes in MEG and LFP power around tremor onset. Twenty-nine tremor epochs from 17 subthalamic nuclei and 10 subjects were included in this analysis. One subject was excluded because tremor onset could not be determined. For seven subthalamic nuclei, more than one epoch was available (average: 2.7, range: 2–6). In these cases, subject-specific time-frequency representations were averaged prior to statistical analysis (see 'Materials and methods').

Figure 2A shows an example of tremor onset (Subject 2, right subthalamic nucleus). In this case, tremor amplitude did not increase linearly over time. Instead, tremor developed in a staged fashion. Stage transitions were reflected by MEG power decreases in the beta band, followed by beta power increases and increases at tremor frequency. An enhancement of LFP power at tremor frequency occurred only in the last stage, when tremor amplitude was maximal.

Figure 2B depicts the time course of group level MEG and LFP power statistically compared to baseline (−9 to 0 s). Please note that time-frequency representations were aligned to individual tremor frequency (f). Following tremor onset, both MEG and LFP power showed a similar pattern: narrow-band power increases at tremor frequency and its first harmonic co-occurred with a decrease in the higher frequencies, corresponding to the beta band (13–30 Hz). For LFP power, the increase at tremor frequency reached significance 4.8 s after tremor onset ($P = 0.01$). MEG power decreased significantly between 10 and 20 Hz relative to tremor frequency in the

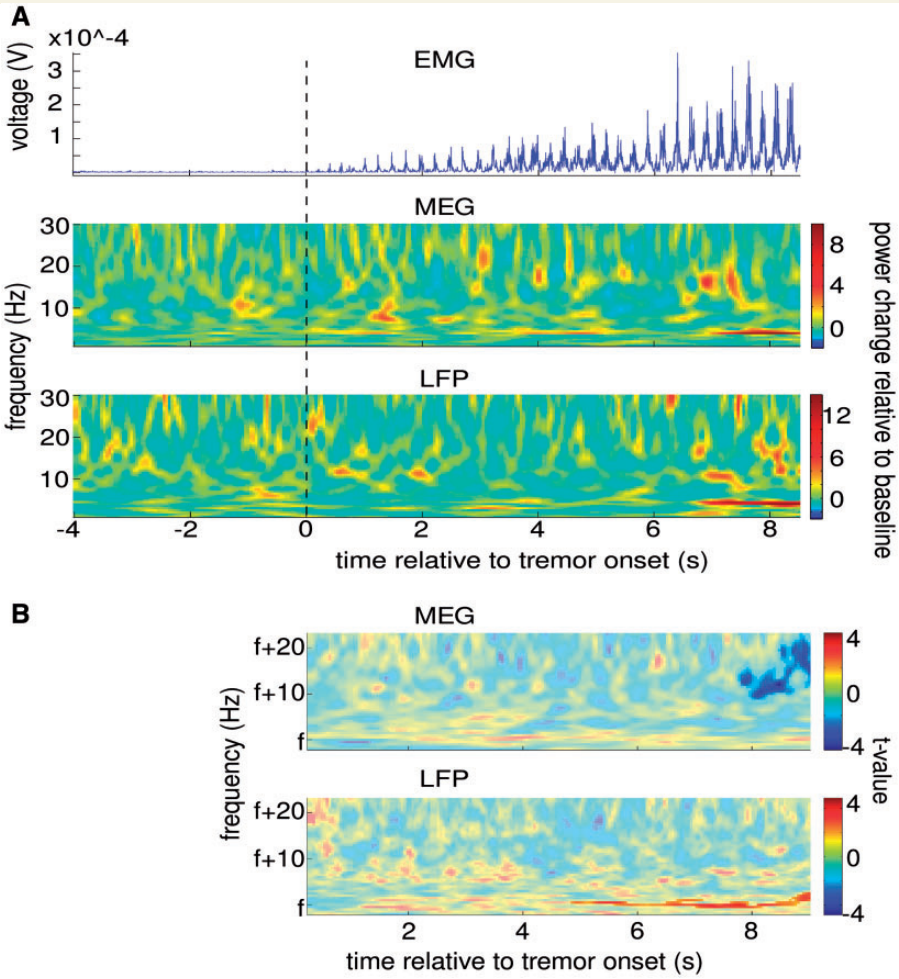

Figure 2 Cortex and subthalamic nucleus showed tremor-related power changes. (**A**) Exemplary data from a tremor phase in Subject 2. The figure shows the rectified EMG signal (*top*), MEG power (*middle*) and LFP power (*bottom*) around tremor onset (dotted line). MEG power was averaged over the sensors of interest. Time-frequency plots were baseline-corrected (baseline: −4 to 0 s) and the relative power change is colour-coded. Note that sudden increases of tremor amplitude are preceded by MEG beta power decreases and followed by power increases at tremor frequency. (**B**) Group statistical image of MEG and LFP power showing the contrast between the period from 0 to 9 s and the baseline period (−9 to 0 s). Time-frequency representations were aligned to individual tremor frequency (f) i.e. individual time-frequency representations were shifted along the frequency axis until the individual tremor frequency reached the 0 Hz position. Significant effects are highlighted by increased colour intensity ($P < 0.05$; $n = 17$) and *t*-values are colour-coded. *Top*: MEG power between 10 and 20 Hz relative to individual tremor frequency (f + 10 − f + 20) decreased gradually. The effect was significant between 8 and 9 s after tremor onset. *Bottom*: Starting ∼1 s after tremor onset, LFP power increased at tremor frequency (f). The effect was significant from 4.8 to 9 s after tremor onset.

period from 8–9 s after tremor onset ($P < 0.01$). Investigation of the original, non-aligned time-frequency representations revealed a corresponding power decrease between 15 and 25 Hz ($P = 0.01$; data not shown). As depicted in Supplementary Fig. 1, this effect was due to a sustained beta power suppression that began around tremor onset and intensified as tremor continued. Group average LFP beta power decreased between −4 and 0 s and increased transiently at tremor onset (Fig. 2B).

Sensor level coherence

As depicted in Fig. 3A, alignment of coherence spectra to individual tremor frequency revealed tremor-related coherence increases between all pairs of signals specifically at tremor frequency (LFP-MEG: $P = 0.02$, EMG-MEG: $P < 0.01$, EMG-LFP: $P = 0.04$). Notably, the tremor-induced change in EMG power was positively correlated with the change in LFP-MEG coherence ($r = 0.50$, $P = 0.03$; Fig 3B). We did not test for correlations between EMG power and LFP-EMG or EMG-MEG coherence since in these cases power changes are likely to cause coherence changes, leading to trivial correlations.

Source level coherence

The sensor level results show that coupling at tremor frequency between subthalamic nucleus, cortex and muscle increases

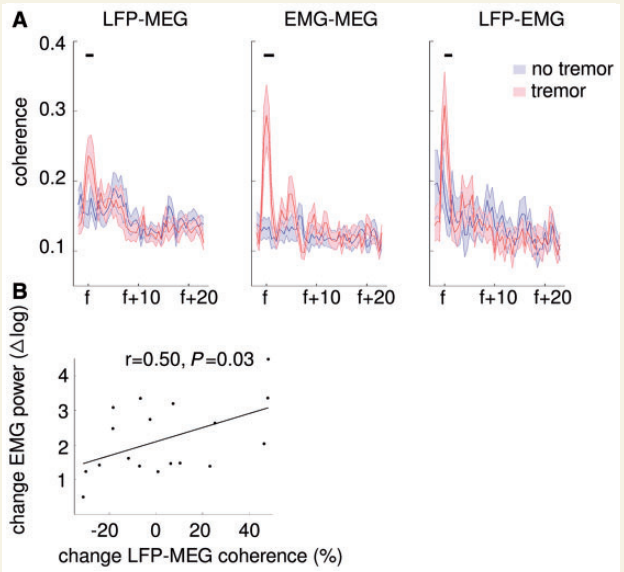

Figure 3 Subthalamic nucleus, cortical motor areas and muscle synchronized during tremor. (**A**) Plots show mean LFP-MEG, EMG-MEG and LFP-EMG coherence in the presence (red) and absence of tremor (blue). Spectra were aligned to individual tremor frequency (f) before averaging. Coherence with MEG was averaged over the sensors of interest. Black, horizontal bars indicate significant differences ($P < 0.05$; $n = 18$). Shaded areas indicate standard error of the mean. (**B**) Changes in LFP-MEG coherence are plotted against changes in EMG power. The line indicates the best linear fit. Values were averaged over the tremor frequency and its first harmonic.

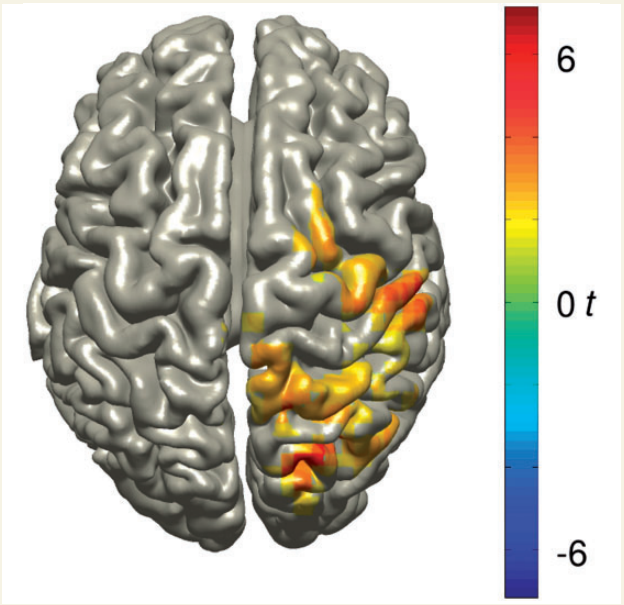

Figure 4 The muscle coupled to a distributed sensorimotor network during tremor. Surface plot illustrates the difference in cortico-muscular coherence between tremor and tremor-free epochs. *t*-values are colour-coded and only significant changes at individual tremor frequency are displayed ($P < 0.05$; $n = 8$). Images depicting right hand tremor (five of eight subthalamic nuclei) were mirrored across the mid-sagittal plane so that the right hemisphere can be considered the hemisphere contralateral to the tremulous limb.

when tremor occurs. To identify the brain areas involved in this process, we computed source level coherence at tremor frequency and contrasted tremor and tremor-free epochs. As the quality of spatial filters depends on the amount of data, we included only subthalamic nuclei for which at least 30 s of rest tremor and 30 s of tremor-free episodes were available. The inclusion criterion was met by eight subthalamic nuclei from six subjects.

Source level analysis revealed significant changes in cortico-muscular but not in subthalamic nucleus-cortex coherence. One cluster was found ($P = 0.02$; Fig. 4), which covered several motor and sensory areas contralateral to tremor. By visual inspection, we identified three local maxima that appeared to be distinct sources. They were located in the primary motor cortex (MNI coordinates: ±60, −15, 50), premotor cortex (MNI coordinates: ±30, 10, 70) and posterior parietal cortex (MNI coordinates: ±20, −75, 50). Supplementary Fig. 2 shows the spatial configuration of selected sources in detail.

Cortico-cortical coupling

To test whether the identified cortical sources are themselves coupled, we estimated their time domain activity and computed ImCoh for all source pairs. In line with previous reports (Timmermann *et al.*, 2003; Pollok *et al.*, 2004), we found cortico-cortical coupling to occur not only at tremor frequency, but also and more frequently at double the tremor frequency. Two representative examples of cortico-cortical coupling are shown in Fig. 5.

A repeated-measures ANOVA with factors 'shuffling' and 'pair' revealed that shifting one signal in time destroyed ImCoh at tremor frequency and its first harmonic. A main effect of shuffling was found when considering tremor epochs [$F(1,7) = 5.95$, $P < 0.05$] and a trend was observed for tremor-free epochs [$F(1,7) = 4.65$, $P = 0.07$]. We found neither a main effect of pair [tremor: $F(2,14) = 0.11$, $P = 0.83$; no tremor: $F(2,14) = 0.04$, $P = 0.94$] nor an interaction between shuffling and pair [tremor: $F(2,14) = 0.58$, $P = 0.57$; no tremor: $F(2,14) = 0.19$, $P = 0.78$]. Rather than affecting coupling between specific pairs of cortical areas, shuffling reduced ImCoh between all pairs to a similar degree (Fig. 6A).

Tremor-related changes in cortico-cortical coupling

The fact that 'shuffling' had a slightly stronger effect in the tremor condition might hint at an influence of tremor on ImCoh. This possibility was not investigated further because a conditional change in ImCoh is difficult to interpret. It may be explained either by a change in phase consistency or by alteration of the

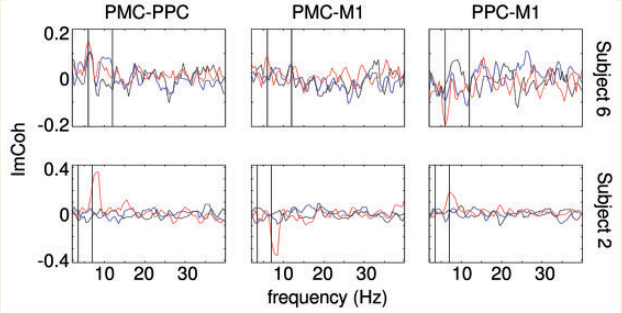

Figure 5 Cortical areas in the tremor network are coupled to one another at tremor frequency and/or double tremor frequency. Plots show examples of ImCoh between pairs of cortical sources from Subject 6 (*top* row) and Subject 2 (*bottom* row). Blue = no tremor; red = tremor; black = shuffled. Vertical lines indicate the tremor frequency and its first harmonic. M1 = primary motor cortex; PPC = parietal cortex; PMC = premotor cortex.

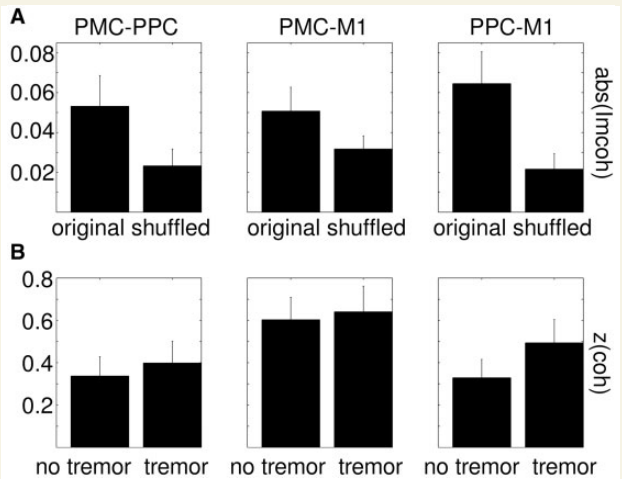

Figure 6 Cortico-cortical coupling increased during tremor. (**A**) Bars represent mean, absolute ImCoh between pairs of cortical sources during tremor ($n = 8$). (**B**) Bars represent mean, *z*-transformed coherence between pairs of cortical sources. Values were averaged over the tremor frequency and its first harmonic. Error bars indicate the standard error of the mean. The *y*-axis scale is the same for all sub-plots within one row. M1 = primary motor cortex; PPC = parietal cortex; PMC = premotor cortex.

preferred phase difference (Gross *et al.*, 2013). As coherence is unaffected by a change in the preferred phase difference, we used coherence to quantify the difference between tremor and tremor-free epochs.

An ANOVA with factors 'tremor' and 'pair' revealed a main effect of tremor [$F(1,7) = 7.48$, $P = 0.03$] and a main effect of pair [$F(2,14) = 5.65$, $P = 0.04$] but no interaction between tremor and pair [$F(2,14) = 1.0$, $P = 0.36$]. As depicted in Fig. 6B, coherence between all pairs increased in the tremor condition. The effect of pair was most likely due to volume conduction, as neighbouring areas exhibited higher coherence than distant areas, regardless of the tremor state.

Discussion

We investigated the parkinsonian rest tremor network by means of simultaneous LFP, MEG and EMG recordings and found that cerebral synchronization at tremor frequency increases as tremor becomes manifest. Increases were observed in a network including subthalamic nucleus, primary motor, premotor and posterior parietal cortex contralateral to the tremulous limb. In addition, we demonstrated that the tremor-associated increase in subthalamic nucleus-cortex coherence was positively correlated with the tremor-associated increase in muscle activity.

Methodological considerations

Simultaneous LFP, MEG and EMG recordings provide unique insights into the relationship between subcortical, cortical and muscle activity in humans and enabled recent advances in the characterization of functional connectivity in Parkinson's disease (Hirschmann *et al.*, 2011, 2013; Litvak *et al.*, 2011, 2012; Oswal *et al.*, 2013). Before discussing the results of the current study in detail, we will consider some methodological aspects associated with coherence measurements obtained with this approach.

One of the major concerns in coherence analysis is the possibility that changes in coherence are trivial consequences of changes in power (Schoffelen and Gross, 2009). Although coherence is normalized by power, it is affected by power changes as they result in changes in the signal-to-noise ratio (Palva and Palva, 2012). In tremor analysis, the most drastic power changes occur in the EMG. Therefore, one might expect EMG power changes to cause changes in cortico-muscular coherence. Importantly, group statistical analysis on the source level excluded this potential confound by demonstrating consistent spatial patterns. Changes in cortico-muscular coherence were consistently observed in a limited set of cortical areas contralateral to the tremulous limb. There is no plausible mechanism by which EMG power changes might affect specifically these areas while sparing all others.

Apart from affecting the signal-to-noise ratio, tremulous movement creates rhythmically changing magnetic fields that may in principle be measured by MEG directly, resulting in artefacts and spurious cortico-muscular coherence. A systematic effect of the latter seems unlikely for the same reasons that speak against confounds because of EMG power changes. Artefacts were rarely observed in this study due to the usage of non-magnetic externalization leads and application of temporal signal space separation.

Finally, imprecise determination of tremor onset could have influenced the results on power time courses. As the emergence of tremor was often gradual, it was not always possible to determine the exact moment of tremor onset. This inevitable imprecision diminished the detection probability of transient effects, since detection requires a high degree of temporal overlap across

epochs. Thus, the analysis was biased towards the detection of sustained effects. Moreover, detection probability increased with time after tremor onset, as any jitter in onset times affected the temporal overlap of sustained effects only in the first seconds after tremor onset.

Subthalamic nucleus and cortical power

In line with previous studies (Levy *et al*., 2002; Liu *et al*., 2002; Wang *et al*., 2006; Reck *et al*., 2009), we observed clear peaks in the subthalamic nucleus LFP power spectra at tremor frequency and double tremor frequency. Moreover, we found a tremor-induced increase of subthalamic nucleus power at individual tremor frequency, as reported in a previous single case study (Wang *et al*., 2005). Notably, the increase occurred several seconds after tremor onset, at a time when tremor amplitude had reached its maximum. Hence, this power increase cannot be the cause of tremor, but could reflect a gradual entrainment of more and more subthalamic nucleus neurons, e.g. by sustained somatosensory feedback (Wang *et al*., 2007; Florin *et al*., 2010). Alternatively, it is conceivable that the detected subthalamic nucleus activity is related to the scale of tremor. Given that the basal ganglia are important for movement scaling (Oliverira *et al*., 1998; Desmurget and Turner, 2010), strong and sustained subthalamic nucleus oscillations might emerge only when tremor amplitude exceeds a certain threshold, i.e. when a large-scale movement is being executed.

In addition to changes at tremor frequency, we found that cortical beta power was suppressed during continuous tremor. This finding tallies with a study in healthy subjects that reported a sustained decrease of cortical beta power during repetitive, voluntary movement (Erbil and Ungan, 2007). Thus, our results further strengthen the claim that voluntary movement and tremor have a common neurophysiological basis (Pollok *et al*., 2004; Schnitzler *et al*., 2006). However, they also provide indications for differences with respect to the dynamics of power. In this study, we did not observe a decrease of cortical beta power before tremor onset, whereas this effect is known to occur before voluntary movement (Pfurtscheller *et al*., 2003). Further studies are needed to elaborate on these potential differences in cortical activity.

Subthalamic nucleus-cortex coherence

While coherence between subthalamic nucleus and EMG at tremor frequency has been addressed by numerous studies (Wang *et al*., 2006; Amtage *et al*., 2008; Reck *et al*., 2009, 2010), subthalamic nucleus-cortex coupling has rarely been investigated in the context of tremor. Importantly, we demonstrated that subthalamic nucleus-cortex coherence increases in the presence of tremor and correlates with tremor severity, showing that: (i) the subthalamic nucleus is part of the central tremor network; and (ii) it generates input to cortex or receives output from cortex that directly reflects tremor amplitude. These findings are complemented by a recent intraoperative study reporting that phase-locking of subthalamic nucleus spikes to motor cortical 6 Hz oscillations is more common in the presence than in the absence of tremor (Shimamoto *et al*., 2013).

The paucity of epochs did not allow for localization of the tremor-associated increase in subthalamic nucleus-cortex coherence observed on the sensor level. Many subjects showed either continuous tremor intermitted by short breaks or short episodes of tremor, resulting in limited amounts of data suited for balanced contrasts and spatial filter construction. Although the amount of epochs sufficed to localize the change in cortico-muscular coherence, localization of the weaker change in subthalamic nucleus-cortex coherence likely requires more or longer recordings.

Cortico-muscular and cortico-cortical coherence

In keeping with previous studies (Volkmann *et al*., 1996; Hellwig *et al*., 2000), we found strong cortico-muscular coherence at tremor frequency and its first harmonic. Coherence increased during epochs of spontaneously emerging rest tremor and the increase could be localized to a set of cortical areas contralateral to the tremulous limb. The fact that increases occurred in both motor and sensory cortical areas suggests that both efferent and afferent rhythmical signalling is enhanced during tremor.

The localization presented in this study closely resembles the tremor network identified in previous MEG (Timmermann *et al*., 2003; Pollok *et al*., 2009) and EEG studies (Muthuraman *et al*., 2012) on parkinsonian tremor. Thus, there is mounting evidence for the existence of a cortical network including primary motor, premotor and posterior parietal cortex that is active during pathological and voluntary tremor (Pollok *et al*., 2004). Interestingly, a recent study revealed the therapeutic potential of modulating the cortical tremor network (Brittain *et al*., 2013). The study demonstrated that interfering with cortical oscillations by transcranial alternating current stimulation over motor cortex leads to substantial tremor alleviation.

In line with the aforementioned studies (Timmermann *et al*., 2003; Pollok *et al*., 2004, 2009), we found that the cortical areas coherent with muscle activity are also coupled to one another. The current results additionally show that cortico-cortical coupling at tremor frequency is dependent on tremor manifestation and is not a trivial consequence of volume conduction.

Comparison with previous studies

Earlier mappings of tremor-related coherence led to the identification of more areas than reported in this study (Timmermann *et al*., 2003; Pollok *et al*., 2004, 2009; Muthuraman *et al*., 2012). In addition to primary motor, premotor and posterior parietal cortex, significant coherence was observed in the supplementary motor area, secondary somatosensory cortex, cerebellum and thalamus. The different results can be explained by differences in methodology. We restricted the analysis to cortical areas to increase statistical power. Furthermore, we used the EMG as reference signal and localized coherence changes (rather than coherence *per se*) in a single step procedure. Previous studies first identified primary motor cortex as the source of maximum coherence with the muscle. Subsequently, the authors searched for sources coherent with primary motor cortex.

Although the approach applied here is less sensitive than the approach used previously, it provides improved reliability. Association with tremor is not based on coherence peaks at tremor frequency but on the contrast between tremor and tremor-free epochs, allowing for the computation of group statistics controlled for multiple comparisons. Moreover, the method does not require removing the activity of strongly coherent sources from the data prior to detection of weaker couplings (Gross *et al*., 2001). This analysis step bears caveats, as incomplete removal will lead to the detection of spurious coupling. Finally, it accounts for the effect of volume conduction. Volume conduction, also referred to as spatial leakage, results from suboptimal spatial filtering and may substantially confound analysis of cortico-cortical connectivity (Schoffelen and Gross, 2009; Palva and Palva, 2012).

Clinical relevance

The current study demonstrates a direct relationship between subthalamic nucleus oscillations at tremor frequency and tremor manifestation. Thus, subthalamic nucleus power and/or subthalamic nucleus-cortex coherence might potentially be used by closed-loop DBS systems designed to suppress tremor. Subthalamic nucleus power is a particularly promising parameter for triggering DBS. In contrast to systems that use cortical action potentials as triggers (Rosin *et al*., 2011), a system using subthalamic nucleus power would not require additional cortical implants and would be robust to slight changes in electrode position. Furthermore, online computation of oscillatory power requires less computational resources than other suggested control parameters, such as phase-amplitude coupling (de Hemptinne *et al*., 2013).

This study provides important information on how subthalamic nucleus power could be used by closed-loop systems. It suggests that power increases at individual tremor frequency could serve as a trigger signal. To achieve more robust tremor detection, we propose to apply DBS whenever subthalamic nucleus power increases at tremor frequency and its first harmonic and simultaneously decreases in the beta band.

Conclusion

Parkinsonian rest tremor is associated with an increase of cerebral synchronization at tremor frequency and double tremor frequency. The increase occurs in a network including subthalamic nucleus, primary motor cortex, premotor cortex and posterior parietal cortex. These results suggest the feasibility of tremor detection based solely on cerebral oscillations.

Acknowledgements

The authors would like to express their sincere gratefulness to the patients who participated in this study. Furthermore, we are very thankful to Medtronic for providing non-magnetic lead extensions. In addition, we thank Mrs. E. Rädisch for assistance with MRI scans.

Funding

This work was supported by ERA-NET Neuron [Neuron-48-013 to A.S.], by the Deutsche Forschungsgemeinschaft [FOR1328, SCHN 592/3-1 to A.S.] and by the European Commission [Marie Curie Fellowship; FP7-PEOPLE-2009-IEF-253965 to M.B.].

Supplementary material

Supplementary material is available at *Brain* online.

References

Amtage F, Henschel K, Schelter B, Vesper J, Timmer J, Lücking C, et al. Tremor-correlated neuronal activity in the subthalamic nucleus of parkinsonian patients. Neurosci Lett 2008; 442: 195–9.

Avants BB, Epstein CL, Grossman M, Gee JC. Symmetric diffeomorphic image registration with cross-correlation: evaluating automated labeling of elderly and neurodegenerative brain. Med Image Anal 2008; 12: 26–41.

Benabid AL, Pollak P, Gervason C, Hoffmann D, Gao DM, Hommel M, et al. Long-term suppression of tremor by chronic stimulation of the ventral intermediate thalamic nucleus. Lancet 1991; 337: 403–6.

Bergman H, Wichmann T, DeLong MR. Reversal of experimental parkinsonism by lesions of the subthalamic nucleus. Science 1990; 249: 1436–8.

Bergman H, Wichmann T, Karmon B, DeLong MR. The primate subthalamic nucleus. II. Neuronal activity in the MPTP model of parkinsonism. J Neurophysiol 1994; 72: 507–20.

Brittain J, Probert-Smith P, Aziz T, Brown P. Tremor suppression by rhythmic transcranial current stimulation. Curr Biol 2013; 23: 436–40.

de Hemptinne C, Ryapolova-Webb ES, Air EL, Garcia PA, Miller KJ, Ojemann JG, et al. Exaggerated phase–amplitude coupling in the primary motor cortex in Parkinson disease. Proc Natl Acad Sci USA 2013; 110: 4780–5.

Deiber MP, Pollak P, Passingham R, Landais P, Gervason C, Cinotti L, et al. Thalamic stimulation and suppression of parkinsonian tremor. Evidence of a cerebellar deactivation using positron emission tomography. Brain 1993; 116 (Pt 1): 267–79.

Desmurget M, Turner RS. Motor aequences and the basal ganglia: kinematics, not habits. J Neurosci 2010; 30: 7685–90.

Deuschl G, Raethjen J, Baron R, Lindemann M, Wilms H, Krack P. The pathophysiology of parkinsonian tremor: a review. J Neurol 2000; 247: V33–48.

Elble RJ. Central mechanisms of tremor. J Clin Neurophysiol 1996; 13: 133–44.

Erbil N, Ungan P. Changes in the alpha and beta amplitudes of the central EEG during the onset, continuation, and offset of long-duration repetitive hand movements. Brain Res 2007; 1169: 44–56.

Florin E, Gross J, Reck C, Maarouf M, Schnitzler A, Sturm V, et al. Causality between local field potentials of the subthalamic nucleus and electromyograms of forearm muscles in Parkinson's disease. Eur J Neurosci 2010; 31: 491–8.

Forstmann BU, Keuken MC, Jahfari S, Bazin P-L, Neumann J, Schäfer A, et al. Cortico-subthalamic white matter tract strength predicts interindividual efficacy in stopping a motor response. Neuroimage 2012; 60: 370–5.

Goetz CG, Tilley BC, Shaftman SR, Stebbins GT, Fahn S, Martinez-Martin P, et al. Movement Disorder Society-sponsored revision of the Unified Parkinson's Disease Rating Scale (MDS-UPDRS): scale presentation and clinimetric testing results. Mov Disord 2008; 23: 2129–70.

Gross J, Baillet S, Barnes GR, Henson R, Hillebrand A, Jensen O, et al. Good practice for conducting and reporting MEG research. Neuroimage 2013; 65: 349–63.

Gross J, Kujala J, Hamalainen M, Timmermann L, Schnitzler A, Salmelin R. Dynamic imaging of coherent sources: studying neural interactions in the human brain. Proc Natl Acad Sci USA 2001; 98: 694–9.

Hammond C, Bergman H, Brown P. Pathological synchronization in Parkinson's disease: networks, models and treatments. Trends Neurosci 2007; 30: 357–64.

Heimer G, Rivlin-Etzion M, Bar-Gad I, Goldberg JA, Haber SN, Bergman H. Dopamine replacement therapy does not restore the full spectrum of normal pallidal activity in the 1-methyl-4-phenyl-1,2,3,6-tetra-hydropyridine primate model of Parkinsonism. J Neurosci 2006; 26: 8101–14.

Hellwig B, Häussler S, Lauk M, Guschlbauer B, Köster B, Kristeva-Feige R, et al. Tremor-correlated cortical activity detected by electroencephalography. Clin Neurophysiol 2000; 111: 806–9.

Helmich RC, Hallett M, Deuschl G, Toni I, Bloem BR. Cerebral causes and consequences of parkinsonian resting tremor: a tale of two circuits? Brain 2012; 135: 3206–26.

Helmich RC, Janssen MJR, Oyen WJG, Bloem BR, Toni I. Pallidal dysfunction drives a cerebellothalamic circuit into Parkinson tremor. Ann Neurol 2011; 69: 269–81.

Hemm S, Coste J, Gabrillargues J, Ouchchane L, Sarry L, Caire F, et al. Contact position analysis of deep brain stimulation electrodes on post-operative CT images. Acta Neurochir 2009; 151: 823–9.

Hirschmann J, Özkurt TE, Butz M, Homburger M, Elben S, Hartmann CJ, et al. Distinct oscillatory STN-cortical loops revealed by simultaneous MEG and local field potential recordings in patients with Parkinson's disease. Neuroimage 2011; 55: 1159–68.

Hirschmann J, Özkurt TE, Butz M, Homburger M, Elben S, Hartmann CJ, et al. Differential modulation of STN-cortical and cortico-muscular coherence by movement and levodopa in Parkinson's disease. Neuroimage 2013; 68: 203–13.

Hoehn MM, Yahr MD. Parkinsonism: onset, progression and mortality. Neurology 1967; 17: 427–42.

Hughes AJ, Daniel SE, Blankson S, Lees AJ. A clinicopathologic study of 100 cases of Parkinson's disease. Arch Neurol 1993; 50: 140–8.

Hurtado JM, Rubchinsky LL, Sigvardt KA, Wheelock VL, Pappas CTE. Temporal Evolution of Oscillations and Synchrony in GPi/Muscle Pairs in Parkinson's Disease. J Neurophysiol 2005; 93: 1569–84.

Hutchison WD, Lozano AM, Tasker RR, Lang AE, Dostrovsky JO. Identification and characterization of neurons with tremor-frequency activity in human globus pallidus. Exp Brain Res 1997; 113: 557–63.

Jenkinson M, Beckmann CF, Behrens TEJ, Woolrich MW, Smith SM. FSL. Neuroimage 2012; 62: 782–90.

Krack P, Pollak P, Limousin P, Benazzouz A, Benabid AL. Stimulation of subthalamic nucleus alleviates tremor in Parkinson's disease. Lancet 1997; 350: 1675.

Kühn AA, Kupsch A, Schneider G-H, Brown P. Reduction in subthalamic 8-35 Hz oscillatory activity correlates with clinical improvement in Parkinson's disease. Eur J Neurosci 2006; 23: 1956–60.

Lang AE, Lozano AM. Parkinson's disease. Second of two parts. N Engl J Med 1998; 339: 1130–43.

Lenz FA, Tasker RR, Kwan HC, Schnider S, Kwong R, Murayama Y, et al. Single unit analysis of the human ventral thalamic nuclear group: correlation of thalamic 'tremor cells' with the 3-6 Hz component of parkinsonian tremor. J Neurosci 1988; 8: 754–64.

Levy R, Ashby P, Hutchison WD, Lang AE, Lozano AM, Dostrovsky JO. Dependence of subthalamic nucleus oscillations on movement and dopamine in Parkinson's disease. Brain 2002; 125: 1196–209.

Litvak V, Eusebio A, Jha A, Oostenveld R, Barnes G, Foltynie T, et al. Movement-related changes in local and long-range synchronization in Parkinson's disease revealed by simultaneous magnetoencephalography and intracranial recordings. J Neurosci 2012; 32: 10541–53.

Litvak V, Jha A, Eusebio A, Oostenveld R, Foltynie T, Limousin P, et al. Resting oscillatory cortico-subthalamic connectivity in patients with Parkinson's disease. Brain 2011; 134: 359–74.

Liu X, Ford-Dunn H, Hayward G, Nandi D, Miall R, Aziz TZ, et al. The oscillatory activity in the parkinsonian subthalamic nucleus investigated using the macro-electrodes for deep brain stimulation. Clin Neurophysiol 2002; 113: 1667–72.

Magariños-Ascone CM, Figueiras-Mendez R, Riva-Meana C, Córdoba-Fernández A. Subthalamic neuron activity related to tremor and movement in Parkinson's disease. Eur J Neurosci 2000; 12: 2597–607.

Maris E, Oostenveld R. Nonparametric statistical testing of EEG- and MEG-data. J Neurosci Methods 2007; 164: 177–90.

Mattout J, Henson RN, Friston KJ. Canonical source reconstruction for MEG. Comput Intell Neurosci 2007; 2007: 1–10.

McAuley JH, Marsden CD. Physiological and pathological tremors and rhythmic central motor control. Brain 2000; 123 (Pt 8): 1545–67.

Moran A, Bergman H, Israel Z, Bar-Gad I. Subthalamic nucleus functional organization revealed by parkinsonian neuronal oscillations and synchrony. Brain 2008; 131: 3395–409.

Mure H, Hirano S, Tang CC, Isaias IU, Antonini A, Ma Y, et al. Parkinson's disease tremor-related metabolic network: characterization, progression, and treatment effects. Neuroimage 2011; 54: 1244–53.

Muthuraman M, Heute U, Arning K, Anwar AR, Elble RJ, Deuschl G, et al. Oscillating central motor networks in pathological tremors and voluntary movements. What makes the difference? NeuroImage 2012; 60: 1331–9.

Nolte G. The magnetic lead field theorem in the quasi-static approximation and its use for magnetoencephalography forward calculation in realistic volume conductors. Phys Med Biol 2003; 48: 3637–52.

Nolte G, Bai O, Wheaton L, Mari Z, Vorbach S, Hallett M. Identifying true brain interaction from EEG data using the imaginary part of coherency. Clin Neurophysiol 2004; 115: 2292–307.

Oliverira RM, Gurd JM, Nixon P, Marshall JC, Passingham RE. Hypometria in Parkinson's disease: automatic versus controlled processing. Mov Disord 1998; 13: 422–7.

Oostenveld R, Fries P, Maris E, Schoffelen J-M. FieldTrip: open source software for advanced analysis of MEG, EEG, and invasive electrophysiological data. Comput Intell Neurosci 2011; 2011: 1–9.

Oswal A, Brown P, Litvak V. Movement related dynamics of subthalmocortical alpha connectivity in Parkinson's disease. Neuroimage 2013; 70: 132–42.

Özkurt TE, Butz M, Homburger M, Elben S, Vesper J, Wojtecki L, et al. High frequency oscillations in the subthalamic nucleus: a neurophysiological marker of the motor state in Parkinson's disease. Exp Neurol 2011; 229: 324–31.

Palva S, Palva JM. Discovering oscillatory interaction networks with M/EEG: challenges and breakthroughs. Trends Cogn Sci (Regul Ed) 2012; 16: 219–30.

Pfurtscheller G, Graimann B, Huggins JE, Levine SP, Schuh LA. Spatiotemporal patterns of beta desynchronization and gamma synchronization in corticographic data during self-paced movement. Clin Neurophysiol 2003; 114: 1226–36.

Pollok B, Gross J, Dirks M, Timmermann L, Schnitzler A. The cerebral oscillatory network of voluntary tremor. J Physiol (Lond) 2004; 554: 871–8.

Pollok B, Makhloufi H, Butz M, Gross J, Chaieb L, Wojtecki L, et al. Levodopa affects functional brain networks in parkinsonian resting tremor. Mov Disord 2009; 24: 91–8.

Raz A, Vaadia E, Bergman H. Firing patterns and correlations of spontaneous discharge of pallidal neurons in the normal and the tremulous 1-methyl-4-phenyl-1,2,3,6-tetrahydropyridine vervet model of parkinsonism. J Neurosci 2000; 20: 8559–71.

Reck C, Florin E, Wojtecki L, Krause H, Groiss S, Voges J, et al. Characterisation of tremor-associated local field potentials in the subthalamic nucleus in Parkinson's disease. Eur J Neurosci 2009; 29: 599–612.

Reck C, Himmel M, Florin E, Maarouf M, Sturm V, Wojtecki L, et al. Coherence analysis of local field potentials in the subthalamic nucleus: differences in parkinsonian rest and postural tremor. Eur J Neurosci 2010; 32: 1202–14.

Rosin B, Slovik M, Mitelman R, Rivlin-Etzion M, Haber SN, Israel Z, et al. Closed-loop deep brain stimulation is superior in ameliorating parkinsonism. Neuron 2011; 72: 370–84.

Schnitzler A, Gross J. Normal and pathological oscillatory communication in the brain. Nat Rev Neurosci 2005; 6: 285–96.

Schnitzler A, Münks C, Butz M, Timmermann L, Gross J. Synchronized brain network associated with essential tremor as revealed by magnetoencephalography. Mov Disord 2009; 24: 1629–35.

Schnitzler A, Timmermann L, Gross J. Physiological and pathological oscillatory networks in the human motor system. J Physiol Paris 2006; 99: 3–7.

Schoffelen J-M, Gross J. Source connectivity analysis with MEG and EEG. Hum Brain Mapp 2009; 30: 1857–65.

Sekihara K, Nagarajan SS, Poeppel D, Marantz A, Miyashita Y. Application of an MEG eigenspace beamformer to reconstructing spatio-temporal activities of neural sources. Hum Brain Mapp 2002; 15: 199–215.

Shimamoto SA, Ryapolova-Webb ES, Ostrem JL, Galifianakis NB, Miller KJ, Starr PA. Subthalamic nucleus neurons are synchronized to primary motor cortex local field potentials in Parkinson's disease. J Neurosci 2013; 33: 7220–33.

Stein JF, Aziz TZ. Does imbalance between basal ganglia and cerebellar outputs cause movement disorders? Curr Opin Neurol 1999; 12: 667–9.

Taulu S, Simola J. Spatiotemporal signal space separation method for rejecting nearby interference in MEG measurements. Phys Med Biol 2006; 51: 1759–68.

Thomson DJ. Spectrum estimation and harmonic analysis. Proc IEEE 1982; 70: 1055–96.

Timmermann L, Gross J, Dirks M, Volkmann J, Freund H-J, Schnitzler A. The cerebral oscillatory network of parkinsonian resting tremor. Brain 2003; 126: 199–212.

Van Veen BD, Buckley KM. Beamforming: a versatile approach to spatial filtering. IEEE ASSP Mag 1988; 5: 4–24.

Volkmann J, Joliot M, Mogilner A, Ioannides AA, Lado F, Fazzini E, et al. Central motor loop oscillations in parkinsonian resting tremor revealed magnetoencephalography. Neurology 1996; 46: 1359–9.

Wang S, Aziz TZ, Stein JF, Bain PG, Liu X. Physiological and harmonic components in neural and muscular coherence in parkinsonian tremor. Clin Neurophysiol 2006; 117: 1487–1498.

Wang S, Aziz TZ, Stein JF, Liu X. Time–frequency analysis of transient neuromuscular events: dynamic changes in activity of the subthalamic nucleus and forearm muscles related to the intermittent resting tremor. J Neurosci Methods 2005; 145: 151–8.

Wang S, Chen Y, Ding M, Feng J, Stein JF, Aziz TZ, et al. Revealing the dynamic causal interdependence between neural and muscular signals in parkinsonian tremor. J Franklin Ins 2007; 344: 180–195.

Zirh TA, Lenz FA, Reich SG, Dougherty PM. Patterns of bursting occurring in thalamic cells during parkinsonian tremor. Neuroscience 1998; 83: 107–21.